ELSEVIER

Journal of Organometallic Chemistry 580 (1999) 48–55

Journal of Organometallic Chemistry

Synthesis, characterization and crystal structures of osmium–rhodium mixed-metal clusters containing pentamethylcyclopentadienyl ligand: $[Os_3Rh(\mu\text{-}CO)_2(CO)_9(\eta^5\text{-}Cp^*)]$, $[Os_3Rh_2(\mu\text{-}H)(\mu\text{-}CO)_2(CO)_8(\eta^5\text{-}Cp^*)(\mu_2\text{-}\eta^5,\eta^1\text{-}CH_2C_5Me_4)]$ and $[Os_3Rh(\mu_3\text{-}H)(\mu\text{-}Cl)(\mu\text{-}CO)(CO)_9(\eta^5\text{-}Cp^*)]$

Sarah Yeuk-Wah Hung, Wing-Tak Wong *

Department of Chemistry, The University of Hong Kong, Pokfulam Road, Hong Kong, PR China

Received 2 September 1998

Abstract

Treatment of the anionic triosmium cluster $[N(PPh_3)_2][Os_3(\mu\text{-}H)(CO)_{11}]$ with one equivalent of $[RhCp^*(MeCN)_3][\{PF_6\}_2]$ [Cp* = pentamethylcyclopentadiene] yielded three Cp*-containing clusters including $[Os_3Rh(\mu\text{-}H)_2(\mu\text{-}CO)(CO)_9(\eta^5\text{-}Cp^*)]$ **1**, $[Os_3Rh(\mu\text{-}CO)_2(CO)_9(\eta^5\text{-}Cp^*)]$ **2** and $[Os_3Rh_2(\mu\text{-}H)(\mu\text{-}CO)_2(CO)_8(\eta^5\text{-}Cp^*)(\mu_2\text{-}\eta^5,\eta^1\text{-}CH_2C_5Me_4)]$ **3**. Solid state vacuum pyrolysis of **2** gave **1** in moderate yield via the replacement of a bridging carbonyl by two bridging hydrides. The coupling reaction of $[N(PPh_3)_2][Os_3(\mu\text{-}H)(CO)_{11}]$ with the monocationic complex, $[RhCp^*(dppe)Cl][PF_6]$ [dppe = bis(diphenylphosphino)ethane] afforded the tetranuclear cluster $[Os_3Rh(\mu_3\text{-}H)(\mu\text{-}Cl)(\mu\text{-}CO)(CO)_9(\eta^5\text{-}Cp^*)]$ **4** in a moderate yield. Clusters **2**–**4** have been fully characterized by both spectroscopic and crystallographic methods. The X-ray structure analysis shows that **3** comprises an edge-bridging tetrahedron in which one of the pentamethylcyclopentadienyl units adopts a novel $\mu_2\text{-}\eta^5,\eta^1$-bonding mode across a Os–Rh bond. Cluster **4** is a tetranuclear osmium–rhodium mixed-metal cluster containing a chloride, bridging across the wing-tips of the butterfly core.

Keywords: Osmium; Rhodium; Clusters; Pentamethylcyclopentadienyl; Carbonyl

1. Introduction

The ionic coupling reaction is a useful and reliable synthetic route for mixed-metal clusters [1–4], even though these reactions may involve redox changes and lead to a complicated mixture of products which are hard to predict or control [5–8].

The stability of the pentamethylcyclopentadienyl-rhodium unit, $\{Rh(\eta^5\text{-}Cp^*)\}$, has been widely studied in mono- and bi-nuclear metal complexes [9]. Shore and co-workers reported that the reactions of $[Os_3(\mu\text{-}H)_2(CO)_{10}]$ with $[Rh(CO)_2(\eta^5\text{-}Cp^*)]$ gave a series of $\{Rh(\eta^5\text{-}Cp^*)\}$ containing mixed-metal clusters, $[Os_3Rh(\mu\text{-}H)_2(CO)_{10}(\eta^5\text{-}Cp^*)]$ and $[Os_2Rh_2(CO)_8(\eta^5\text{-}Cp^*)]$, which are interconvertible under appropriate conditions [10]; whereas a hexanuclear mixed-metal cluster, $[Os_5Rh(CO)_{15}(\eta^5\text{-}Cp^*)]$, was isolated by Lewis, Johnson and co-workers, from the reaction of $[\{N(PPh_3)_2\}_2][Os_5(CO)_{15}]$ with $[RhCp^*(MeCN)_3][\{SbF_6\}_2]$ [11]. In addition, a closely related series of RuRh systems are also known [12,13].

To gain more understanding of this system and to expand the utility of the coupling approach, this paper reports the reactions of $[N(PPh_3)_2][Os_3(\mu\text{-}H)(CO)_{11}]$ with the rhodium capping reagents, $[RhCp^*(MeCN)_3][\{PF_6\}_2]$ and $[RhCp^*(dppe)Cl][PF_6]$, to produce a number of new osmium–rhodium carbonyl clusters.

* Corresponding author. Fax: +852-2547-2933.
E-mail address: chemmail@hkucc.hku.hk (W.-T. Wong)

PII: S0022-328X(98)01094-8

2. Results and discussion

The reaction of $[N(PPh_3)_2][Os_3(\mu\text{-}H)(CO)_{11}]$ with $[RhCp^*(MeCN)_3][\{PF_6\}_2]$ in dichloromethane at ambient conditions for 1 h gave a known cluster, $[Os_3Rh(\mu\text{-}H)_2(\mu\text{-}CO)(CO)_9(\eta^5\text{-}Cp^*)]$ **1** [10], and two new osmium–rhodium carbonyl cluster complexes, $[Os_3Rh(\mu\text{-}CO)_2(CO)_9(\eta^5\text{-}Cp^*)]$ **2** and $[Os_3Rh_2(\mu\text{-}H)(\mu\text{-}CO)_2(CO)_8(\eta^5\text{-}Cp^*)(\mu_2\text{-}\eta^5,\eta^1\text{-}CH_2C_5Me_4)]$ **3**. Cluster **2** could be converted into **1** as the major product via vacuum pyrolysis at 140°C; the formation of other minor products in this pyrolytic reaction is the hydride source for cluster **1**. However, the attempted carbonylation of **1** does not regenerate **2**. On the other hand, the coupling product $[Os_3Rh(\mu_3\text{-}H)(\mu\text{-}Cl)(\mu\text{-}CO)(CO)_9(\eta^5\text{-}Cp^*)]$ **4** was formed in the reaction of $[N(PPh_3)_2][Os_3(\mu\text{-}H)(CO)_{11}]$ with $[RhCp^*(dppe)Cl][PF_6]$ in a 25% yield (Scheme 1). The three new products **2**–**4** were characterized by both spectroscopic and crystallographic techniques.

2.1. Spectroscopic analyses of complexes **2**–**4**

The spectroscopic data (IR, ^{1}H-NMR and MS) in Table 1 for the new compounds, **2**–**4**, are fully consistent with the solid-state structures established by X-ray diffraction study. The IR spectra of complexes **2**–**4** show strong absorption bands in the region of 1600–2200 cm^{-1} due to terminal carbonyl stretchings. In addition, relatively weak signals are observed at 1624 and 1620 cm^{-1} due to bridging carbonyls for complex **2**, and 1712 cm^{-1} for complex **3**. The mass spectrum of **3** gives a characteristic isotopic pattern, which confirm the presence of transition metals. Specifically, complex **3** is expected to contain the largest number of transition metal atoms. Complexes **2** and **4** should be of the same nuclearity as their mass numbers range from *m*/*z* 1117 to 1125.

Based on the results of the structural analyses of compounds (vide infra), the ^{1}H-NMR signals are assigned to the appropriate protons. The presence of a η^5-terminally bonded Cp* fragments in all complexes is evidenced by ^{1}H-NMR spectroscopy. For complex **3**, the five additional signals at δ 1.71, 1.58, 1.52, 1.44 and 1.25 ppm, with an integral ratio of 2:3:3:3:3, are ascribed to methyl protons of the $\{\eta^2\text{-}CH_2CMe_4\}$ unit. The broad singlet at δ 1.71 ppm is assigned to the methylene group protons which are coordinated directly to an osmium metal. It is noteworthy that upfield signals due to metal hydrides are observed at δ -12.64

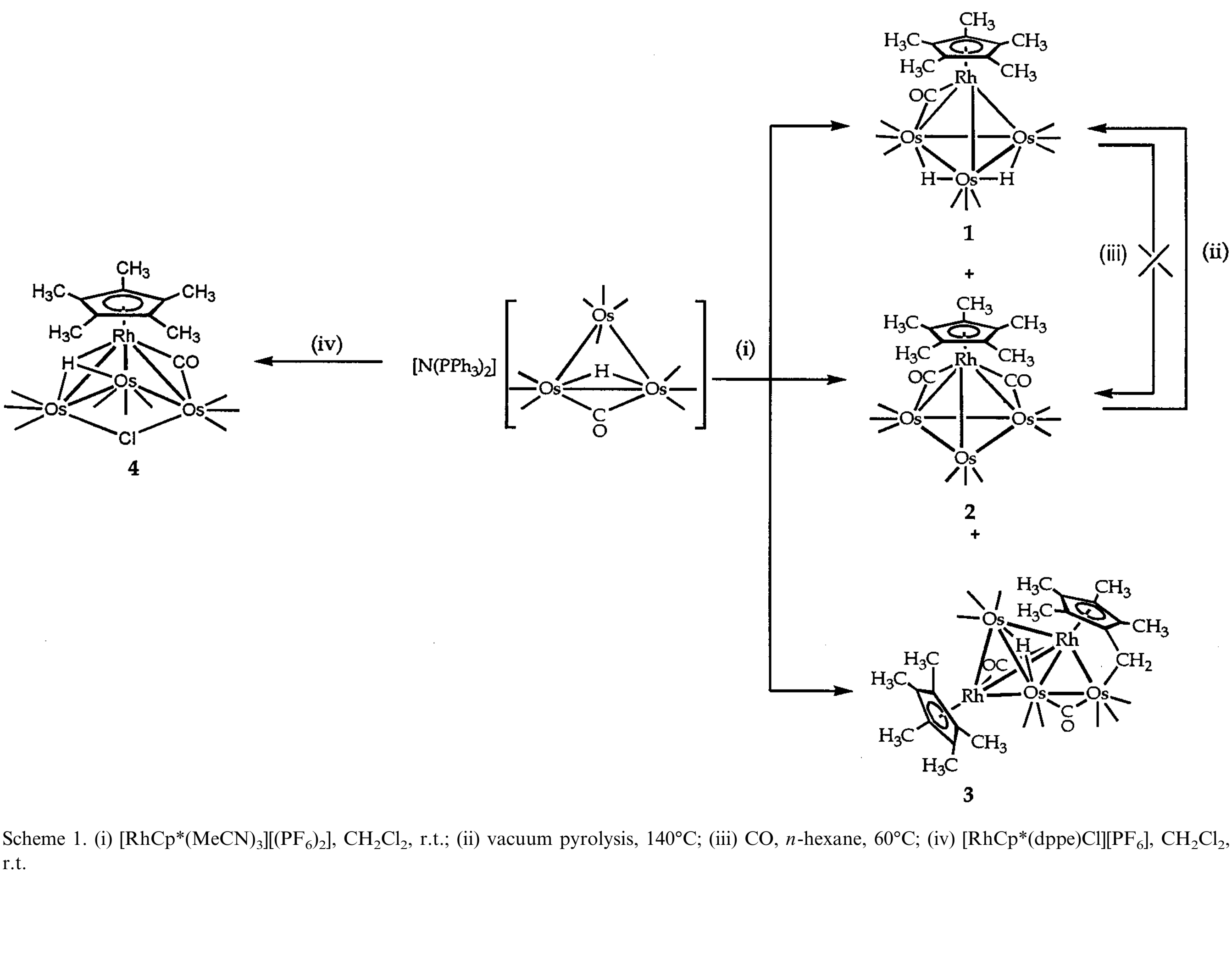

Scheme 1. (i) $[RhCp^*(MeCN)_3][(PF_6)_2]$, CH_2Cl_2, r.t.; (ii) vacuum pyrolysis, 140°C; (iii) CO, *n*-hexane, 60°C; (iv) $[RhCp^*(dppe)Cl][PF_6]$, CH_2Cl_2, r.t.

Table 1
Spectroscopic data for clusters **2**–**4**

Compound	IR(ν_{CO})[a] (cm^{-1})	^{1}H-NMR[b] (ppm)	MS[c] (m/z)
2	2076m, 2032s, 2001w, 1983m, 1962w, 1624m, 1620m	2.19 [s, 15H, Cp*]	1117, (1116)
3	2078m, 2068m, 2055w, 2035m, 2028s, 2016m, 2003m, 1995w, 1989w, 1712m	2.17 [s, 15H, Cp*], 1.71 [s, 2H, CH_2], 1.58 [s, 3H, CH_3], 1.52 [s, 3H, CH_3], 1.44 [s, 3H, CH_3], 1.25 [s, 3H, CH_3], −12.64 [s, 1H, MH]	1325, (1326)
4	2103m, 2066s, 2043w, 2024s, 2003w, 1991m, 1964w, 1823m	1.57 [s, 15H, Cp*], −14.06 [d, 1H, $J_{RhH}=17$, MH]	1125, (1125)

[a] Recorded in n-hexane.
[b] Recorded in $CDCl_3$, J values in Hz.
[c] Positive FAB MS, calculated values in parentheses.

and −14.06 ppm in the spectra for **3** and **4**, respectively.

The multiplicity of hydride signals is useful for its assignment. Rhodium has a non-zero spin the same as a proton (^{103}Rh spin = 1/2, 100% natural abundance). If a metal hydride spans the heterometallic bond (Os–Rh), the signal should be observed as a doublet or multiplet with a coupling constant of J_{RhH}. On the other hand, the hydride across the Os–Os bond should result in a singlet [10,14,15]. Hence a singlet signal in **3** can be viewed as the hydride bridging homometallic Os–Os edge while the doublet signal observed in complex **4** is attributed to hydride bonded directly to a rhodium atom. The spectroscopic evidence discussed so far does not allow definitive assignments for positions of the {Rh(η^5-Cp*)} caps and the structures of the compounds; thus X-ray crystallographic analysis has to be carried out on each of them.

*2.2. Crystallographic analyses of complexes **2**–**4***

Bright red crystals of **2** suitable for structural analysis were grown by slow evaporation of pure n-hexane solution. The crystal structure of **2** together with some bond parameters are shown in Fig. 1 and Table 2, respectively. The molecule is based upon a closed tetrahedral Os_3Rh unit. The usual 60 valence electrons are associated with a tetrahedral array similar to the closely related compounds [$Os_3M(\mu\text{-}H)_2(\mu\text{-}CO)(CO)_9(\eta^5\text{-}Cp)$] (M = Co, Rh or Ir) [16]. There exists a crystallographic imposed mirror symmetry defined by the metal atoms, Rh(1) and Os(1), and the mid-point of the Os(2)–Os(2*) bond. Each osmium atom is linked to three terminal carbonyl ligands and two unsymmetrical bridging carbonyl groups are found across the Os(2)–Rh(1) and Os(2*)–Rh(1) bonds. The bond separation of Rh(1)–C(6) (2.21(2) Å) is significantly longer than the Os(2)–C(6) bond (2.04(2) Å) which results from the steric effect of the pentamethylated Cp* ligand at the rhodium vertex. Within the triosmium base, the Os–Os bond distances are in a range of 2.7788(6) to 2.8297(8) Å, which are similar to those observed in [$Os_3(CO)_{12}$] [17]. On the other hand, the unbridged Os–Rh bond distance (2.749(1) Å) is comparable to the corresponding mean value in [$Os_3Rh(\mu\text{-}H)_2(\mu\text{-}CO)(CO)_9(\eta^5\text{-}Cp^*)$] **1** (2.730 Å) [10], but the two bridging Os–Rh edges in **2** are relatively long (2.809(1) Å).

An X-ray crystallographic study was undertaken on a dark purple single crystal obtained from a CH_2Cl_2/n-hexane solution of **3**. A perspective view of **3** is shown in Fig. 2. Selected interatomic distances and angles are listed in Table 3. The metal core of **3** can be viewed as an edge-bridged tetrahedron in which no formal bonding is found between the Os(1) and Os(3) atoms [Os(1)···Os(3) = 4.15 Å]. Such metal disposition has been observed in [$Os_4Pt(\mu\text{-}H)_2(CO)_{15}$] [18]. For the two rhodium atoms of **3**, each carries a η^5-pentamethylcyclopentadienyl ring. In contrast to the intact Cp* on the Rh(1) atom, C–H bond activation is observed on the {$\mu\text{-}CH_2C_5Me_4$} ligand bridging an Os(3)–Rh(2) bond. This ring is in a η^5-bonding mode to the Rh(2) atom with one of the methyl groups directly bonded to an osmium atom [Os(3)–C(30), 2.20(3) Å]. Such metallation on C(30) accounts for the shortening effect of the C(25)–C(30) bond [1.35(3) Å]. A similar bridging arene system has been observed in [$Os_4(CO)_{11}(C_5Me_4CH_2)$] [19]. It is worth pointing out that the Os–Rh bond distances in **3** (2.688(2)–2.852(2) Å) spans a wider range than those in complex **2** (2.749(1)–2.809(1) Å). The longer bond of Os(3)–Rh(2) in **3** can be attributed to the existence of a bulky pentamethylcyclopentadienyl bridge. The average Os–Os bond length is 2.837(1) Å, in which Os(1)–Os(2) (2.852(1) Å) is 0.03 Å longer than the Os(2)–Os(3) bond (2.822(1) Å). The hydride ligand in **3** has been located from potential energy calculations. It bridges the Os(1)–Os(2) edge which is only slightly longer than Os(2)–Os(3) separation. Normally, a hydride increases the metal–metal bond length by at least 0.1 Å, this effect is obscured in compound **3** because of the carbonyl bridge across Os(2)–Os(3). A symmetrical bridge, C(6)–O(6), is observed spanning the Os(2)–Os(3) vector [Os(2)–C(6), 1.89(2) Å; Os(3)–

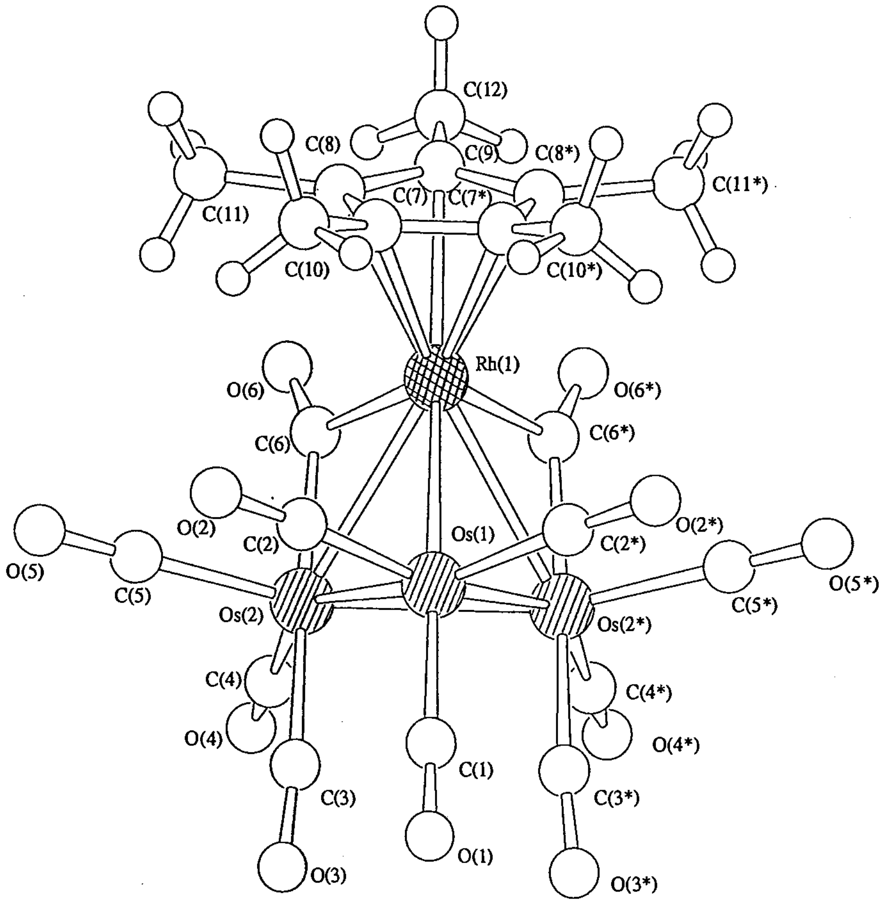

Fig. 1. Molecular structure of cluster **2** showing the atomic numbering scheme for non-hydrogen atoms.

C(6), 2.48(3) Å]. Another bridging carbonyl resides on the Rh(1)–Rh(2) bond (2.730(2) Å), and this rhodium–rhodium bond distance compares well with the one found in the complex $[Os_2Rh_2(\mu\text{-}H)_2(CO)_7(\eta^5\text{-}Cp^*)_2]$ (2.712(1) Å) which is also bridged by one carbonyl ligand [10]. The molecule contains a total of 74 cluster valence electrons which is the value expected for a edged bridged tetrahedron according to the EAN rule.

Brown crystals of **4** of good X-ray quality were grown from a saturated CH_2Cl_2/*n*-hexane solution of the complex. The molecular structure of the tetranuclear, mixed-metal cluster $[Os_3Rh(\mu_3\text{-}H)(\mu\text{-}Cl)(\mu\text{-}CO)(CO)_9(\eta^5\text{-}Cp^*)]$ **4** and selected interatomic distances and angles are given in Fig. 3 and Table 4, respectively. The solid state structure is composed of an Os_3Rh butterfly metal framework where the rhodium carrying a $\{\eta^5\text{-}Cp^*\}$ unit is positioned at the hinge site. There is a chloride group asymmetrically bridging the wing-tip atoms, Os(1) and Os(3) [Os(1)–Cl(1) = 2.465(6) Å; Os(3)–Cl(1) = 2.458(7) Å]. A similar bridging wing-tip butterfly has been observed in $[Os_4(\mu\text{-}H)_3(\mu\text{-}I)(CO)_{12}]$ [20], $[Os_3Ir(\mu\text{-}H)_2(\mu\text{-}Cl)(CO)_{12}]$ [21] and $[Ru_4(\mu\text{-}Cl)(CO)_{13}]^-$ [22]. The dihedral angle between the Os(1), Os(2), Rh(1) and Os(2), Os(3), Rh(1) planes in the metal framework is 88.57°. There are five metal–metal bonds including two homometallic Os–Os bonds and three heterometallic Os–Rh vectors. The Os–Rh bonds can be sub-divided into a hinge bond, Os(2)–Rh(1), and two wing edges, Os(1)–Rh(1) and Os(3)–Rh(1). The former, Os(2)–Rh(1) (2.749(2) Å), is slightly shorter than the other two Os–Rh bonds [Os(1)–Rh(1), 2.787(2) Å; Os(3)–Rh(1), 2.791(2) Å]. A μ_3-hydride is located by potential energy calculations on the Rh(1), Os(2), Os(3) face so that the two wing edges, Os(3)–Rh(1) and Os(2)–Os(3), are found to be longer than the Os(1)–Rh(1) and Os(2)–Os(1) bonds, respectively.

Table 2
Selected bond distances (Å) and angles (°) for cluster **2**

Bond distance			
Os(1)–Os(2)	2.7788(6)	Os(1)–Os(2*)	2.7788(6)
Os(2)–Os(2*)	2.8297(8)	Os(1)–Rh(1)	2.749(1)
Os(2)–Rh(1)	2.809(1)	Os(2)–C(6)	2.04(2)
Rh(1)–C(6)	2.21(2)		
Bond angle			
Os(2)–Os(1)–Os(2*)	61.22(2)	Os(1)–Os(2)–Os(2)*	59.39(1)
Os(1)–Rh(1)–Os(2)	59.99(2)		

* Symmetry code: *x*, 1/2 − *y*, *z*.

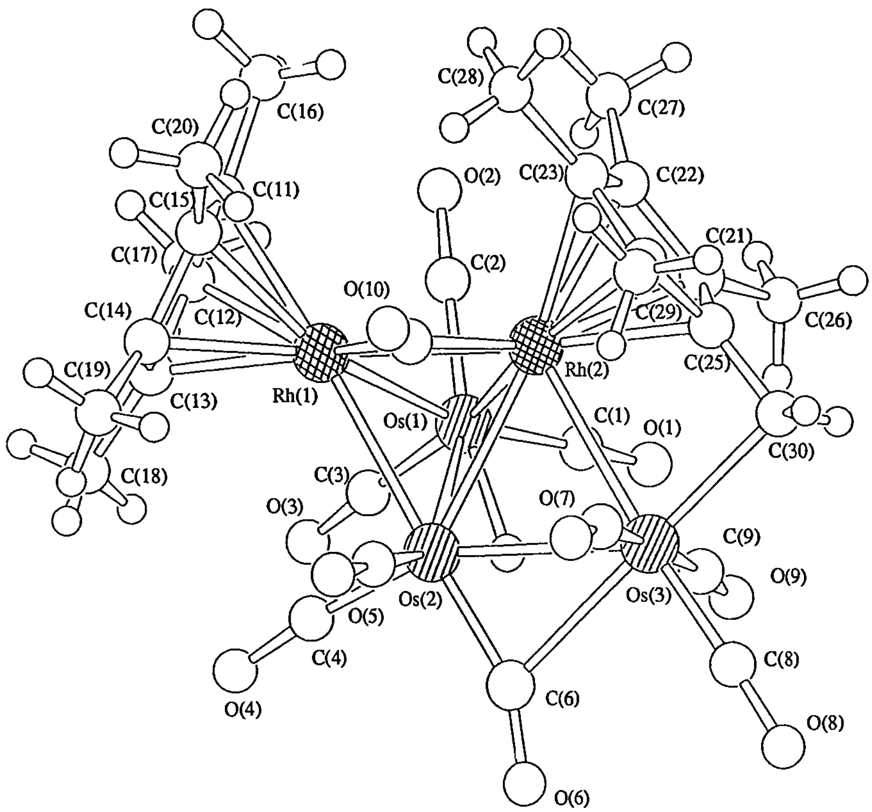

Fig. 2. Molecular structure of cluster **3** showing the atomic numbering scheme for non-hydrogen atoms.

With respect to the *closo*-tetrahedron of complex **2**, the open butterfly structure of **4** releases the steric constraint imposed by the pentamethylcyclopentadienyl group; hence the carbonyl ligand bridging the Os(1)–Rh(1) bond in **4** bends towards the rhodium vertex [Os(1)–C(4), 2.21(2) Å; Rh(1)–C(4), 1.87(2) Å]. In total nine additional carbonyl groups are terminally bonded to the osmium atoms so that cluster **4** is electron precise which can be rationalized by the EAN rule.

3. Experimental

All reactions and manipulations were carried out under an inert atmosphere using standard Schlenk techniques. Solvents were purified by standard procedures and freshly distilled prior to use. All chemicals, except where stated, were purchased commercially and used as received. The complexes $[N(PPh_3)_2][Os_3(\mu\text{-}H)(CO)_{11}]$ [23], $[RhCp^*(MeCN)_3][\{PF_6\}_2]$ [24] and $[RhCp^*(dppe)Cl][PF_6]$ [25] were prepared following the literature methods. IR spectra were recorded on a Bio-Rad FTS-7 IR spectrometer, using 0.5 mm calcium fluoride solution cells. Proton NMR spectra were recorded at 25°C on a Bruker DPX 300, using CD_2Cl_2 and referenced to $SiMe_4$ (δ 0). Mass spectra were recorded on a Finnigan MAT 95 instrument by the fast atom bombardment technique, using *m*-nitrobenzyl alcohol or α-thioglycerol as the matrix solvents. Microanalyses were performed by Butterworth Laboratories, UK. Routine purification of products was carried out in air by thin-layer chromatography on plates coated with Merck Kieselgel 60 GF_{254}.

3.1. Reaction of $[N(PPh_3)_2][Os_3(\mu\text{-}H)(CO)_{11}]$ with $[RhCp^*(NCMe)_3][\{PF_6\}_2]$

A solution of $[N(PPh_3)_2][Os_3(\mu\text{-}H)(CO)_{11}]$ (50 mg, 0.035 mmol) in CH_2Cl_2 (20 cm^3) was stirred with $[RhCp^*(NCMe)_3][\{PF_6\}_2]$ (23 mg, 0.035 mmol) at room temperature (r.t.) under a nitrogen atmosphere. The

Table 3
Selected bond distances (Å) and angles (°) for cluster **3**

Bond distance			
Os(1)–Os(2)	2.852(1)	Os(2)–Os(3)	2.822(1)
Os(1)–Rh(1)	2.688(2)	Os(1)–Rh(2)	2.713(2)
Os(2)–Rh(1)	2.786(2)	Os(2)–Rh(2)	2.781(2)
Os(3)–Rh(2)	2.852(2)	Rh(1)–Rh(2)	2.730(2)
Os(2)–C(6)	1.89(2)	Os(3)–C(6)	2.48(3)
Os(3)–C(30)	2.20(3)	Rh(1)–C(10)	2.00(2)
Rh(2)–C(10)	1.93(2)	C(25)–C(30)	1.35(3)
Bond angle			
Os(1)–Os(2)–Os(3)	94.01(3)	Os(1)–Rh(1)–Os(2)	62.76(4)
Os(1)–Rh(2)–Os(2)	62.53(4)	Rh(1)–Os(1)–Rh(2)	60.71(5)
Rh(1)–Os(2)–Rh(2)	58.74(5)		

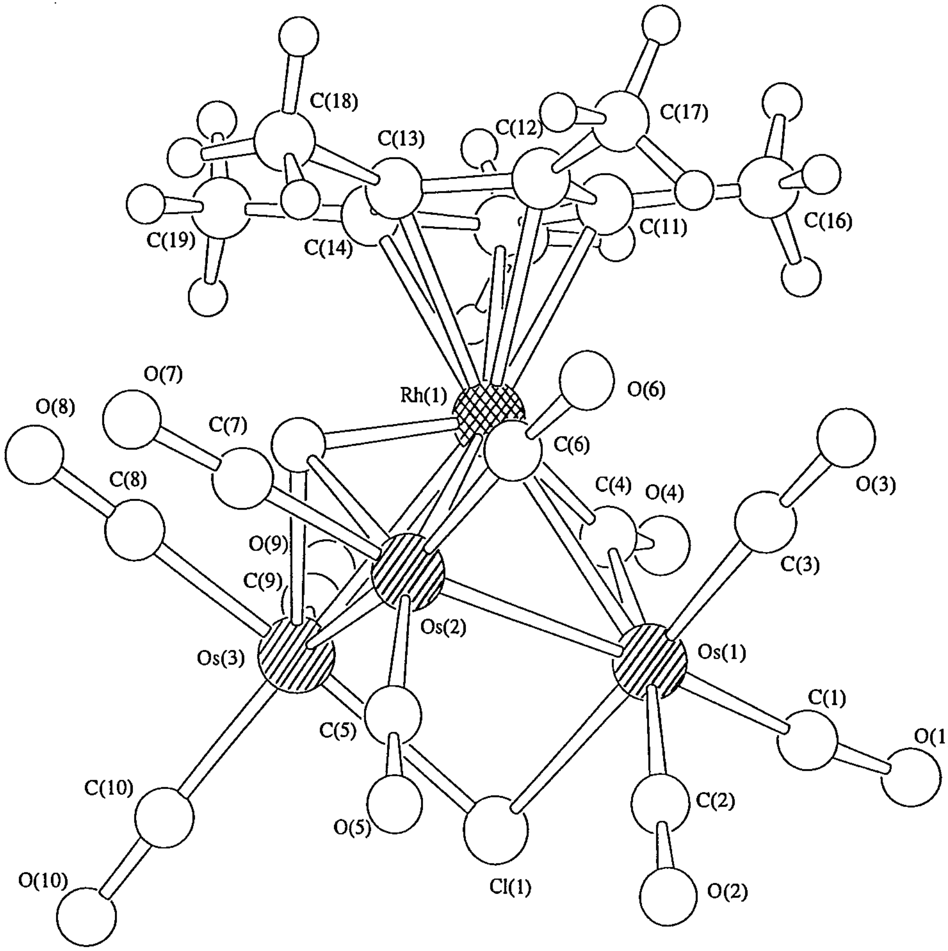

Fig. 3. Molecular structure of cluster **4** showing the atomic numbering scheme for non-hydrogen atoms.

initial red solution immediately changed to brown upon stirring. After 30 min the mixture was then concentrated by reduced pressure and purified by TLC using the eluent of n-hexane/CH_2Cl_2 (3:1, v/v) to afford three bands, namely cluster products [$Os_3Rh(\mu\text{-}H)_2(\mu\text{-}CO)(CO)_9(\eta^5\text{-}Cp^*)$] **1** ($R_f$ ca. 0.75, 10 mg, 26%), [$Os_3Rh(\mu\text{-}CO)_2(CO)_9(\eta^5\text{-}Cp^*)$] **2** ($R_f$ ca. 0.5, 8 mg, 20%) and [$Os_3Rh_2(\mu\text{-}H)(\mu\text{-}CO)_2(CO)_8(\eta^5\text{-}Cp^*)(\mu_2\text{-}\eta^5,\eta^1\text{-}CH_2C_5Me_4)$] **3** ($R_f$ ca. 0.35, 6 mg, 12%). (Found: C, 22.63; H, 1.41. Calc. for $C_{21}H_{15}O_{11}Os_3Rh$ **2**: C, 22.58; H, 1.34. Found: C, 27.17; H, 2.32. Calc. for $C_{30}H_{30}O_{10}Os_3Rh_2$ **3**: C, 27.15; H, 2.26%).

3.2. Vacuum pyrolysis of [$Os_3Rh(\mu\text{-}CO)_2(CO)_9(\eta^5\text{-}Cp^*)$] 2

A concentrated CH_2Cl_2 solution (ca. 4 cm^3) of **2** (30 mg, 0.027 mmol) was added into a Carius tube. The solvent was removed under reduced pressure and the tube was sealed after being dried. The tube was then placed in a preheated silicone oil bath at 140°C for 5 min to give a dark brown solid. The dark residue was extracted with CH_2Cl_2 and the combined extract, after being concentrated was subjected to preparative TLC separation. Elution with n-hexane/CH_2Cl_2, (3:1, v/v) afforded [$Os_3Rh(\mu\text{-}H)_2(\mu\text{-}CO)(CO)_9(\eta^5\text{-}Cp^*)$] **1** ($R_f$ ca. 0.75, 30%) in addition to a number of uncharacterized minor products.

Table 4
Selected bond distances (Å) and angles (°) for cluster **4**

Bond distance			
Os(1)–Os(2)	2.838(1)	Os(2)–Os(3)	2.904(1)
Os(1)–Rh(1)	2.787(2)	Os(2)–Rh(1)	2.749(2)
Os(3)–Rh(1)	2.791(2)	Os(1)–Cl(1)	2.465(6)
Os(3)–Cl(1)	2.458(7)	Os(1)–C(4)	2.21(2)
Rh(1)–C(4)	1.87(2)		
Bond angle			
Os(2)–Os(1)–Rh(1)	58.50(4)	Os(2)–Os(3)–Rh(1)	57.69(4)
Os(1)–Os(2)–Rh(1)	59.82(4)	Os(1)–Rh(1)–Os(2)	61.68(5)
Os(1)–Cl(1)–Os(3)	92.0(2)		

Table 5
Crystallographic data and data collection parameters for complexes **2**–**4**

Compound	**2**	**3**	**4**
Empirical formula	$C_{21}H_{15}O_{11}Os_3Rh$	$C_{30}H_{30}O_{10}Os_3Rh_2$	$C_{20}H_{16}O_{10}ClOs_3Rh$
Molecular weight	1116.85	1326.97	1125.30
Crystal size (mm)	0.25 × 0.21 × 0.21	0.19 × 0.24 × 0.25	0.12 × 0.22 × 0.22
Crystal system	Monoclinic	Orthorhombic	Monoclinic
Space group	$P2_1/m$ (no. 11)	$P2_12_12_1$ (no. 19)	$P2_1/n$ (no. 14)
Unit cell dimensions			
a (Å)	8.827(1)	10.967(1)	9.761(4)
b (Å)	14.797(1)	16.188(1)	16.069(4)
c (Å)	9.894(1)	18.414(2)	16.264(4)
α (°)	90.0	90.0	90.0
β (°)	105.22(2)	90.0	92.46(3)
γ (°)	90.0	90.0	90.0
V (Å^3)	1247.0(2)	3269.1(4)	2548(1)
Z	2	4	4
D_{calc} (g cm^{-3})	2.974	2.696	2.933
$F(000)$	1004	2432	2024
Diffractometer	Marresearch Image Plate	Marresearch Image Plate	Rigaku-AFC7R
μ (cm^{-1})	159.32	126.51	156.9
Reflections collected	12144	20041	3717
Unique reflections	2398	3462	3481
Observed reflections [$I>3\sigma(I)$]	2071	2963	1710
p in weighting scheme	0.024	0.024	0.005
R indices (observed data)	$R=0.046$, $R'=0.057$	$R=0.046$, $R'=0.054$	$R=0.033$, $R'=0.031$
Goodness-of-fit	1.74	1.95	1.48
Largest Δ/σ	0.03	0.02	0.05
No. of parameters	167	206	166
Residual extrema in the final difference map (close to Os) (e Å^{-3})	2.13 to −2.80	1.40 to −2.62	1.04 to −0.76

*3.3. Carbonylation of [$Os_3Rh(\mu$-$H)_2(\mu$-$CO)(CO)_9(\eta^5$-$Cp^*)$] **1***

A stream of CO gas was bubbled through a n-hexane solution (60 cm^3) containing [$Os_3Rh(\mu$-$H)_2(\mu$-$CO)(CO)_9(\eta^5$-$Cp^*)$] **1** (30 mg, 0.028 mmol). However, no chemical change occurred even though the mixture was heated to reflux for 5 h.

3.4. Reaction of [$N(PPh_3)_2$][$Os_3(\mu$-$H)(CO)_{11}$] with [$RhCp^*(dppe)Cl$][PF_6]

To a solid mixture of [$N(PPh_3)_2$][$Os_3(\mu$-$H)(CO)_{11}$] (50 mg, 0.035 mmol) and [$RhCp^*(dppe)Cl$][PF_6] (29 mg, 0.035 mmol), a degassed CH_2Cl_2 (20 cm^3) was added. The colour of the resultant solution turned from red to brown within 5 min. The solvent was evaporated in vacuo and the dark brown residue was purified by preparative TLC using n-hexane/CH_2Cl_2, (1:1, v/v) as eluent. Trace amounts of compounds were unidentified. A brown band with R_f ca. 0.5 was characterized as [$Os_3Rh(\mu_3$-$H)(\mu$-$Cl)(\mu$-$CO)(CO)_9(\eta^5$-$Cp^*)$] **4** (10 mg, 25%). (Found: C, 21.32; H, 1.44. Calc. for $C_{20}H_{16}O_{10}ClOs_3Rh$ **4**: C, 21.33; H, 1.42%).

4. Crystallography

All pertinent crystallographic data and other experimental details are summarized in Table 5. Data were collected at ambient temperature either on a MAR research image plate scanner (complexes **2** and **3**) or Rigaku AFC7R diffractometer (complex **4**), using Mo–K$_\alpha$ radiation ($\lambda = 0.71073$ Å) with a graphite-crystal monochromator in the incident beam. For **2** and **3**, 65 3° frames with an exposure time of 5 min per frame were used, for **4**, all the data were collected using the ($\omega - 2\theta$) scan technique with a scan rate of 16.00 min^{-1} (in ω). The diffracted intensities were corrected for Lorentz and polarisation effects. The ψ-scan method was employed for semi-empirical absorption corrections for **4**, however, an approximation to absorption correction by inter-image scaling was made for **2** and **3**. Scattering factors were taken from Ref. [26a] and anomalous dispersion effects [26b] were included in F_c.

The structures were solved by direct methods (SIR 88) [27] and expanded by Fourier-difference techniques. The solutions were refined on F by full-matrix least-squares analysis with Os and Rh atoms refined anisotropically. The hydrides for complexes **3** and **4** were located on the Fourier-difference map using low-angle data and were also estimated by potential energy calculations [28]. All the hydrogen atoms are included in the structure factor calculations but the parameters were not refined. Calculations were performed on a Silicon-Graphics computer, using the program package TEXSAN [29].

Atomic coordinates, thermal parameters, bond lengths and angles have been deposited at the Cambridge Crystallographic Data Centre (CCDC).

Acknowledgements

W.-T. Wong gratefully acknowledges financial support from the University of Hong Kong. S.Y.-W. Hung acknowledges the receipt of a postgraduate studentship and Hung Hing Ying scholarships administered by the University of Hong Kong.

References

[1] D.E. Fjare, W.L. Gladfelter, J. Am. Chem. Soc. 106 (1984) 4799.
[2] J. Lewis, C.A. Morewood, P.R. Raithby, M.C.R. Arellano, J. Chem. Soc. Dalton Trans. (1997) 3335.
[3] J.E. Davies, S. Nahar, P.R. Raithby, G.P. Shields, J. Chem. Soc. Dalton Trans. (1997) 13.
[4] J.W.S. Hui, W.T. Wong, J. Organomet. Chem. 524 (1996) 211.
[5] S.Y.W. Hung, W.T. Wong, J. Chem. Soc. Chem. Commun. (1997) 2099.
[6] M.A. Beswick, J. Lewis, P.R. Raithby, M.C.R. Arellano, Angew. Chem. Int. Ed. Engl. 36 (1997) 291.
[7] A. Fumagalli, S. Martinengo, G. Ciani, G. Marturano, Inorg. Chem. 25 (1986) 592.
[8] R.D. Pergola, L. Garlaschelli, F. Demartin, M. Manassero, N. Masciocchi, J. Chem. Soc. Dalton Trans. (1988) 201.
[9] P.M. Maitlis, Chem. Soc. Rev. 10 (1981) 1.
[10] D.Y. Jan, L.Y. Hsu, W.L. Hsu, S.G. Shore, Organometallics 6 (1987) 274.
[11] R.K. Henderson, P.A. Jackson, B.F.G. Johnson, J. Lewis, P.R. Raithby, Inorg. Chim. Acta 198 (1992) 393.
[12] W.E. Lindsell, C.B. Knobler, H.D. Kaesz, J. Organomet. Chem. 296 (1985) 209.
[13] A. Colomobie, D.G. McCarthy, J. Krause, L.G. Hsu, W.L. Hsu, D.Y. Yan, S.G. Shore, J. Organomet. Chem. 421 (1990) 383.
[14] A. Colombie, D.A. McCarthy, J. Krause, L.Y. Hsu, W.L. Hsu, D.Y. Jan, S.G. Shore, J. Organomet. Chem. 383 (1990) 421.
[15] E.G. Lundquist, J.C. Huffman, K. Folting, B.E. Mann, K.G. Caulton, Inorg. Chem. 29 (1990) 128.
[16] L.Y. Hsu, W.L. Hsu, D.A. McCarthy, J.A. Krause, L.H. Chung, S.G. Shore, J. Organomet. Chem. 426 (1992) 121.
[17] M.R. Churchill, B.G. DeBoer, Inorg. Chem. 16 (1977) 878.
[18] R.D. Adams, M.P. Pompeo, W. Wu, Inorg. Chem. 30 (1991) 2899.
[19] W. Wang, H.B. Davis, F.W.B. Einstein, R.K. Pomeroy, Organometallics 13 (1994) 5133.
[20] B.F.G. Johnson, J. Lewis, P.R. Raithby, K. Wong, J. Chem. Soc. Dalton Trans. (1980) 1248.
[21] C.J. Farrugia, A.G. Orpen, F.G.A. Stone, Polyhedron 2 (1983) 171.
[22] G.R. Steinmetz, A.D. Harley, G.L. Geoffroy, Inorg. Chem. 19 (1980) 2985.
[23] E.W. Abel, M.A. Bennett, G. Wilkinson, J. Chem. Soc. (1959) 3178.
[24] C. White, S.J. Thompson, P.M. Maitlis, J. Chem. Soc. Dalton Trans. (1977) 1654.
[25] J.W. Kang, K. Moseley, P.M. Maitlis, J. Am. Chem. Soc. (1969) 5970.
[26] D.T. Cromer, J.T. Waber, International Tables for X-Ray Crystallography, vol. 4, Kynoch Press, Birmingham, 1974: (a) Table 2.2B; (b) Table 2.3.1.
[27] M.C. Burla, M. Camalli, G. Cascarnao, C. Giacovazzo, G. Polidor, R. Spagna, D. Viterbo, SIR 88, J. Appl. Crystallogr. 22 (1989) 389.
[28] A.G. Orpen, J. Chem. Soc. Dalton Trans. (1980) 2509.
[29] TEXSAN, Crystal Structure Analysis Package, Molecular Structure Corporation, Houston, TX, 1985 and 1992.